

hep-ph/0602022

November 15, 2018

USING INVISIBLE GRAVITON RADIATION TO DETECT HEAVY ELECTROWEAK RESONANCES AT A 500 GeV e^+e^- COLLIDER

Sreerup Raychaudhuri and Saswati Sarkar

Department of Physics, Indian Institute of Technology, Kanpur 208 016, India.

Electronic address: sreerup@iitk.ac.in, saswati_05@gmail.com

ABSTRACT

The process $e^+e^- \rightarrow \mu^+\mu^- E_T$, where the missing energy is due to the production of a tower of invisible graviton states in a model with large extra dimensions, is considered. We focus on the scenario when this process is used to detect a heavy dileptonic resonance in the electroweak sector of the model, taking as example some models with an extra Z' boson. It turns out that at a 500 GeV machine with 1000 fb^{-1} of luminosity, it may be possible to use this process to detect such resonances if there are two large extra dimensions and the string scale is not too far above a TeV.

A concerted international effort is currently under way to build a high energy linear e^+e^- collider, which, in the wake of expected discoveries at the LHC, would conduct *precision* experiments to probe the TeV scale. While discussions on the technical design and feasibility of such a machine are already under way[1], it is essential, at the moment, to study the physics possibilities of such a facility and to determine what would be the best options to have when the experimental design is finalized. Quite naturally, the study of such physics possibilities[2] is heavily dependent on the experience of the past, where the LEP collider was specifically designed to refine and complement the discoveries made with the proton synchrotron at CERN. The difference, in this case, is that we have no unique prediction of the discoveries expected at the LHC, and hence, the design for a linear collider must be broad-based and robust enough to adjust to all contingencies.

Ever since the first serious accelerator experiments in the 1960s, resonance hunting has always been a major concern of any high energy experiment. A hadron collider is an ideal machine for seeking resonances, as the natural variations in parton momenta provide a wide spread of effective centre-of-mass energies, which then allow the machine to pick up any unknown resonances within its kinematic reach. This is not the case at an e^+e^- collider, where the initial state energies are fixed and have to be decided as part of the machine design. This feature has obvious advantages for precision measurements, as, for example, at LEP-1, where the energy was fine-tuned to the Z^0 resonance, but there is always the possibility that there may exist an unknown resonant state which lies several decay widths away from the actual machine energy, and consequently, produces a very small effect. A major concern at a linear e^+e^- collider, would, therefore, be the identification of ways and means of ‘seeing’ such resonances. This can be achieved if there is a mechanism to *spread out* the initial state energies. Fortunately, a mechanism is readily at hand, namely initial-state radiation and beamstrahlung, producing either hard, transverse photons (which can be tagged) or soft, collinear photons which will go unobserved down the beam pipe creating a mismatch in the observed momentum balance in the longitudinal direction[3].

In this work, we consider a different – and somewhat more exotic – possibility, namely, that the electroweak physics at a TeV is embedded in a large-extra-dimensions model of the kind introduced by Arkani-Hamed, Dimopoulos and Dvali (ADD) in 1998[4]. This model would then consist of some simple extension (with dileptonic resonances) of the Standard Model confined on the ‘brane’ – a four-dimensional hypersurface embedded in a $4+d$ dimensional ‘bulk’ – with massless gravitons free to propagate in the bulk. On the brane, where laboratory experiments must be conducted, the gravitons will appear as multitudes of massive spin-2

Kaluza-Klein states, each coupling very weakly to matter and gauge fields, but collectively building up to near-electroweak strengths in e^+e^- collisions. We focus on the possibility of radiative processes, where each emitted graviton escapes detection (because of its extremely weak coupling to matter) and leads to missing energy and momentum signals. In this paper, to be specific, we have considered the possibility that an electroweak resonance, like an extra Z' boson, for example, could be excited in a simple process like

$$e^+e^- \rightarrow \mu^+\mu^- \cancel{E}_T$$

where the missing energy (\cancel{E}_T) due to escaping *gravitons* provides the spread in the effective centre-of-mass energy necessary to home in on the Z' resonance. However, it may be pointed out at this very stage that a dileptonic resonance need not necessarily be an extra Z' boson – it could very well be a scalar, a tensor or an exotic spin state which are readily obtained in TeV-scale string theories[5].

Irrespective of the specific electroweak model with a Z' boson (provided the Z' couples to e^+e^- and $\mu^+\mu^-$), there are seven diagram topologies contributing, at the lowest order, to the process $e^+e^- \rightarrow \mu^+\mu^- G_n$, with exchange of, respectively, a photon, a Z boson or a Z' boson, i.e. 21 Feynman diagrams in all. These follow from the basic s -channel boson-exchange diagram shown in Fig. 1, with the possibility of a graviton state being radiated, not just from an initial state (as shown), but from any one of the five internal or external legs or from any one of the two vertices. One can safely neglect the corresponding diagrams where a graviton (or a tower of gravitons) is exchanged in place of the neutral gauge bosons, since the corresponding amplitudes will be very small¹.

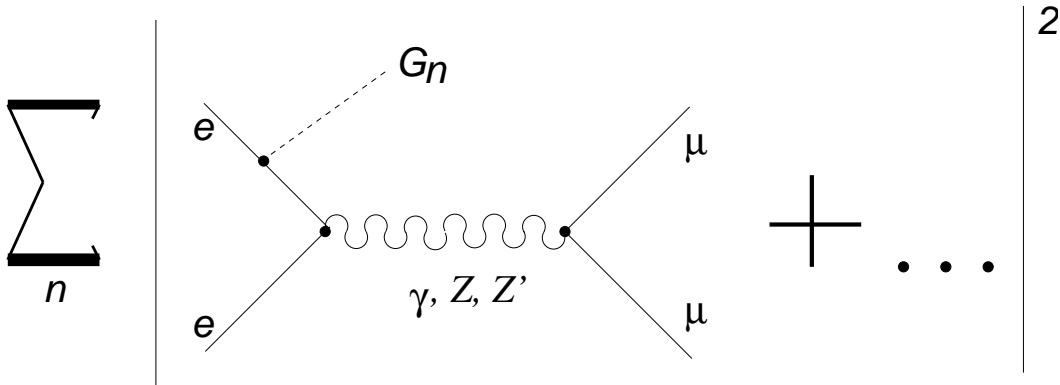


Figure 1. *Feynman diagrams contributing to the process $e^+e^- \rightarrow \mu^+\mu^- G_n$.*

It is necessary to make a coherent sum of all 21 diagrams to obtain the cross-section

$$\sigma_n(M_n) = \sigma(e^+e^- \rightarrow \mu^+\mu^- G_n)$$

¹Suppressed by four extra powers of M_s , the string scale, which will be a TeV or more.

with radiation of a particular graviton Kaluza-Klein mode G_n . The Feynman rules are given in Refs. [6, 7]. The entire calculation, though straightforward, is long and tedious. We have performed these calculations by evaluating all the trace relations using the software FORM[8]. Each graviton contributes separately to the missing energy signal, which means that we require to make an incoherent sum over all graviton states which are kinematically accessible, i.e.

$$\sigma = \sum_n \sigma_n(M_n) \simeq \int_0^{\sqrt{s}} dM \rho(M) \sigma(M)$$

making the quasi-continuum approximation for the closely-spaced graviton states. The density-of-states function $\rho(M)$ is given in Ref. [7]. The actual cross-sections are calculated by inserting the squared, spin-summed matrix elements into a Monte Carlo event generator, which provides numerical results of the required degree of accuracy. In this article we present only the physics results.

In our numerical analysis, we have implemented the following kinematic cuts:

1. The final state muons should not be too close to the beam pipe, which is ensured by demanding that the muon pseudorapidity should satisfy $\eta_\mu < 2.5$ for both the muon tracks.
2. The muons should also have significant transverse momentum, which is ensured by demanding that $p_T^\mu > 10$ GeV for both muon tracks.
3. There should be substantial missing energy, which is ensured by demanding that $\cancel{p}_T > 20$ GeV. It is also useful to impose an upper cut $\cancel{p}_T < 200$ GeV to get rid of photon-exchange processes where the muons are very soft.
4. The dimuon invariant mass $M_{\mu\mu} = (p_{\mu^+} + p_{\mu^-})^2$, which should show a peak at the Z' resonance, should satisfy $M_{\mu\mu} > 200$ GeV which not only removes the peaks due to the photon and Z -exchange effects, but also reduces the SM background² substantially. It may be noted that we would not miss out on resonances in the 100–200 GeV range because these are already ruled out by LEP-2 data.

For the graviton masses and couplings, we have adopted the minimal ADD model, which is characterised by two parameters, viz. the number of compact dimensions d and the (so-called) string scale M_S . The constraints on M_S from purely terrestrial experiments[9] vary between about 0.7–1.2 TeV, depending on d . We have, in general, chosen $M_S \geq 1$ TeV. In this paper,

²Here 'SM background' refers to the SM embedded in an ADD-type scenario.

in keeping with the general philosophy of laboratory-based analyses, we choose to ignore the strong astrophysical bounds[10] on the $d = 2$ scenario.

There is a much wider choice when it comes to deciding the parameters of the Z' sector. In general, we can write the couplings of the Z' boson to fermions (f) as

$$\mathcal{L}_{int}^{Z'f\bar{f}} = \bar{\Psi}_f \gamma^\mu \left[g_{Lf}^{\prime(n)} P_L + g_{Rf}^{\prime(n)} P_R \right] \Psi_f Z'_\mu \quad (1)$$

where $P_{L/R} = \frac{1}{2}(1 \mp \gamma_5)$ and $g_{Lf}^{\prime(n)}$ and $g_{Rf}^{\prime(n)}$. The couplings of the Z' boson to chiral fermions are different for each scenario (n) considered. In order to have a focussed discussion, we have chosen to follow the pragmatic approach of Dittmar *et al* [11] which is limited to just five scenarios, of which the first three are unrealistic and the last two are well motivated.

1. The couplings of the Z' boson are identical with those of the Z boson; the only difference lies in the mass M'_Z . The $\ell^+\ell^-Z'$ vertex (where $\ell = e, \mu$) is given by $g_{L\ell}^{\prime(1)} \simeq -0.20$ and $g_{R\ell}^{\prime(1)} \simeq 0.17$.
2. The coupling of the Z' boson is purely vectorlike, with the vector coupling equal to that of the Z boson; the mass M'_Z is again a free parameter. The $\ell^+\ell^-Z'$ vertex has $g_{L\ell}^{\prime(2)} \simeq -0.20$ and $g_{R\ell}^{\prime(2)} = 0$.
3. The coupling of the Z' boson is purely axial, with the axial coupling equal to that of the Z boson; as before, the mass M'_Z is a free parameter. The $\ell^+\ell^-Z'$ vertex has $g_{L\ell}^{\prime(3)} = 0$ and $g_{R\ell}^{\prime(3)} \simeq 0.17$.
4. The Z' boson arises in a $SU(2)_L \times U(1)_Y \times U(1)_{Y'}$ model which originates in the spontaneous breakdown of an E_6 group:

$$\begin{aligned}
& E_6 \\
& \downarrow \\
& SO(10) \times U(1)_\psi \\
& \downarrow \\
& SU(5) \times U(1)_\psi \\
& \downarrow \\
& SU(3)_c \times SU(2)_L \times U(1)_Y \times U(1)_{Y'} \\
& \downarrow \\
& SU(3)_c \times SU(2)_L \times U(1)_Y \\
& \downarrow \\
& SU(3)_c \times U(1)_{em}
\end{aligned}$$

In this model, there are two Z' -bosons. We focus on the lighter Z' , which is a mixture $Z' = Z'_\chi \cos \beta + Z'_\psi \sin \beta$, where β varies between $-\pi/2$ to $+\pi/2$, with $\beta = -\tan^{-1} \sqrt{5/3} \simeq -0.91$ corresponding to direct breaking of E_6 in superstring-inspired models, with no intermediate $SO(10)$ group. The $\ell^+ \ell^- Z'$ vertex now has $g_{L\ell}^{\prime(4)} \simeq 0.238 \cos(\beta - 0.406)$ and $g_{R\ell}^{\prime(4)} \simeq -0.119 \sin(\beta - 0.659)$.

5. The Z' boson arises in a left-right symmetric model based on a gauged $SU(2)_L \times SU(2)_R \times U(1)_{B-L}$ symmetry, with a much simpler breakdown chain

$$\begin{aligned}
& SU(3)_c \times SU(2)_L \times SU(2)_R \times U(1)_{B-L} \\
& \quad \downarrow \\
& \quad SU(3)_c \times SU(2)_L \times U(1)_Y \\
& \quad \downarrow \\
& \quad SU(3)_c \times U(1)_{em}
\end{aligned}$$

which is presumably the end sector of the breakdown of a bigger symmetry which unifies colour interactions with the electroweak sector. In this model, the $\ell^+ \ell^- Z'$ vertex has $g_{L\ell}^{\prime(5)} \simeq \frac{0.179}{\alpha_{LR}}$ and $g_{R\ell}^{\prime(5)} \simeq \frac{0.179}{\alpha_{LR}} (1 - \alpha_{LR}^2)$. where the parameter α_{LR} lies between $\sqrt{2/3} \simeq 0.8165$ and $\sqrt{2} \simeq 1.4142$.

In terms of these parameters, we can write the partial decay width of the Z' boson to a pair of fermions as

$$\Gamma_{f\bar{f}}^{(n)} = N_c \frac{M'_Z}{24\pi} \sqrt{1-4x} \left[\left(g_{Lf}^{\prime(n)} \right)^2 + \left(g_{Rf}^{\prime(n)} \right)^2 - x \left\{ \left(g_{Lf}^{\prime(n)} \right)^2 + \left(g_{Rf}^{\prime(n)} \right)^2 - 6 g_{Lf}^{\prime(n)} g_{Rf}^{\prime(n)} \right\} \right] \theta(1-4x) \quad (2)$$

where $x = (m_f/M'_Z)^2$ and N_c is the number of colours of the fermion f . Since, in general, $M'_Z > 100$ GeV from the LEP-2 constraints, we can neglect x for all but the top quark and get a simplified form

$$\Gamma_{f\bar{f}}^{(n)} \simeq N_c \frac{M'_Z}{24\pi} \left[\left(g_{Lf}^{\prime(n)} \right)^2 + \left(g_{Rf}^{\prime(n)} \right)^2 \right] \quad (3)$$

The detailed couplings of the Z' to fermions in these five scenarios are given in Table 1.

(n)	(f)	$g_{Lf}^{(n)}$	$g_{Lf}^{(n)}(\text{num})$	$g_{Rf}^{(n)}$	$g_{Rf}^{(n)}(\text{num})$
(1)	ν	$\frac{g}{2c_W}$	0.372	0	0
	ℓ	$\frac{g}{c_W} \left(s_W^2 - \frac{1}{2} \right)$	-0.201	$\frac{g}{c_W} s_W^2$	0.171
	u	$\frac{g}{2c_W} \left(1 - \frac{4}{3} s_W^2 \right)$	0.258	$-\frac{2g}{3c_W} s_W^2$	-0.114
	d	$\frac{g}{3c_W} \left(s_W^2 - \frac{3}{2} \right)$	-0.315	$\frac{g}{3c_W} s_W^2$	0.057
(2)	ν	$\frac{g}{4c_W}$	0.186	$\frac{g}{4c_W}$	0.186
	ℓ	$\frac{g}{c_W} \left(s_W^2 - \frac{1}{4} \right)$	-0.015	$\frac{g}{c_W} \left(s_W^2 - \frac{1}{4} \right)$	-0.015
	u	$\frac{g}{4c_W} \left(1 - \frac{8}{3} s_W^2 \right)$	0.072	$\frac{g}{4c_W} \left(1 - \frac{8}{3} s_W^2 \right)$	0.072
	d	$\frac{g}{3c_W} \left(s_W^2 - \frac{3}{2} \right)$	-0.129	$\frac{g}{3c_W} \left(s_W^2 - \frac{3}{2} \right)$	-0.129
(3)	ν	$\frac{g}{4c_W}$	0.186	$-\frac{g}{4c_W}$	-0.186
	ℓ	$-\frac{g}{4c_W}$	-0.186	$\frac{g}{4c_W}$	0.186
	u	$\frac{g}{4c_W}$	0.186	$-\frac{g}{4c_W}$	-0.186
	d	$-\frac{g}{4c_W}$	-0.186	$\frac{g}{4c_W}$	0.186
(4)	ν	$\frac{2e}{3c_W} \cos \left(\beta - \tan^{-1} \sqrt{\frac{5}{27}} \right)$	0.238 $\cos(\beta - 0.406)$	0	0
	ℓ	$\frac{2e}{3c_W} \cos \left(\beta - \tan^{-1} \sqrt{\frac{5}{27}} \right)$	0.238 $\cos(\beta - 0.406)$	$-\frac{e}{3c_W} \sin \left(\beta - \tan^{-1} \sqrt{\frac{3}{5}} \right)$	-0.119 $\sin(\beta - 0.659)$
	u	$\frac{e}{3c_W} \sin \left(\beta - \tan^{-1} \sqrt{\frac{3}{5}} \right)$	0.119 $\sin(\beta - 0.659)$	$-\frac{e}{3c_W} \sin \left(\beta - \tan^{-1} \sqrt{\frac{3}{5}} \right)$	-0.119 $\sin(\beta - 0.659)$
	d	$\frac{e}{3c_W} \sin \left(\beta - \tan^{-1} \sqrt{\frac{3}{5}} \right)$	0.119 $\sin(\beta - 0.659)$	$-\frac{2e}{3c_W} \cos \left(\beta - \tan^{-1} \sqrt{\frac{5}{27}} \right)$	-0.238 $\cos(\beta - 0.406)$
(5)	ν	$\frac{e}{2c_W} \frac{1}{\alpha_{LR}}$	$\frac{0.1785}{\alpha_{LR}}$	0	0
	ℓ	$\frac{e}{2c_W} \frac{1}{\alpha_{LR}}$	$\frac{0.1785}{\alpha_{LR}}$	$\frac{e}{2c_W} \frac{1}{\alpha_{LR}} (1 - \alpha_{LR}^2)$	$\frac{0.1785}{\alpha_{LR}} (1 - \alpha_{LR}^2)$
	u	$-\frac{e}{6c_W} \frac{1}{\alpha_{LR}}$	$-\frac{0.0595}{\alpha_{LR}}$	$-\frac{e}{6c_W} \frac{1}{\alpha_{LR}} (1 - 3\alpha_{LR}^2)$	$-\frac{0.0595}{\alpha_{LR}} (1 - 3\alpha_{LR}^2)$
	d	$-\frac{e}{6c_W} \frac{1}{\alpha_{LR}}$	$-\frac{0.0595}{\alpha_{LR}}$	$-\frac{e}{6c_W} \frac{1}{\alpha_{LR}} (1 + 3\alpha_{LR}^2)$	$-\frac{0.0595}{\alpha_{LR}} (1 + 3\alpha_{LR}^2)$

Table 1. *Couplings of the Z' boson to different fermions in the five models under consideration. We write $c_W = \cos \theta_W$ and $s_W = \sin \theta_W$.*

It is now vital to numerically evaluate the total decay width of the Z' boson in these models and determine if, indeed, it will appear as a narrow resonance. This is illustrated in Figure 2, where we have plotted the total decay width $\Gamma_{Z'}$ as a function of $M'_{Z'}$ for different values of the couplings in the two realistic models in question, i.e. (4) and (5). The hatched area corresponds to the E_6 model, i.e. (4), while the dotted area corresponds to the left-right symmetric model, i.e. (5). These areas have been generated by varying the couplings β and α_{LR} over the full allowed range (see above). The three solid lines show the width in the (unrealistic) comparison models (1), (2) and (3). Small deviations from linearity in all the curves correspond to opening-up of the $t\bar{t}$ decay channel. The dark-shaded area is ruled out by the direct LEP-2 constraints.

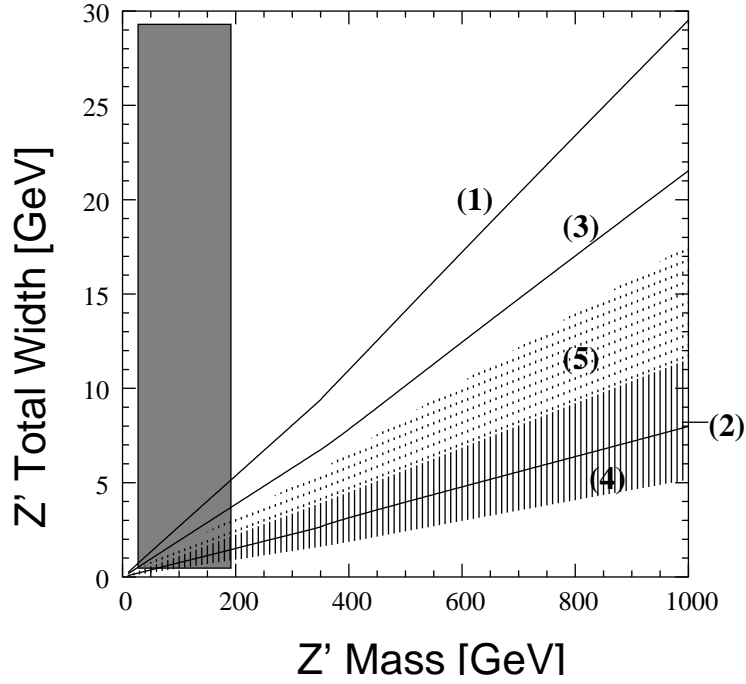


Figure 2. Decay width of the Z' boson in five different models as a function of its mass. Numbers in parentheses correspond to the number of the model as described in the text. The dark-shaded region is ruled out by LEP-2.

It may be seen that in the two realistic models (4) and (5), the decay width of the Z' boson does not rise above 17 GeV, even when the mass reaches 1 TeV. Since this indicates $\Gamma_{Z'}/M_{Z'} < 2\%$, we may safely conclude that the Z' -boson will appear as a narrow resonance in the discussion that follows.

In any of the above models, the probability of exciting a Z' resonance in the process $e^+e^- \rightarrow \mu^+\mu^-G_n$ will depend on the probability of emitting initial-state gravitons carrying away the requisite energy from the electron-positron pair. This means that the size of the resonant cross-section will depend rather sensitively on the ADD parameters, viz., d , the number of compact dimensions, and M_S , the string scale. This is illustrated in Figure 3, where we plot the total cross-section as a function of M_S , for a fixed set of all the other parameters, mostly chosen to get a high cross-section. Models 2 and 3 yield cross-sections in the same ballpark as Model 1, and have been omitted to avoid making the figure clumsy.

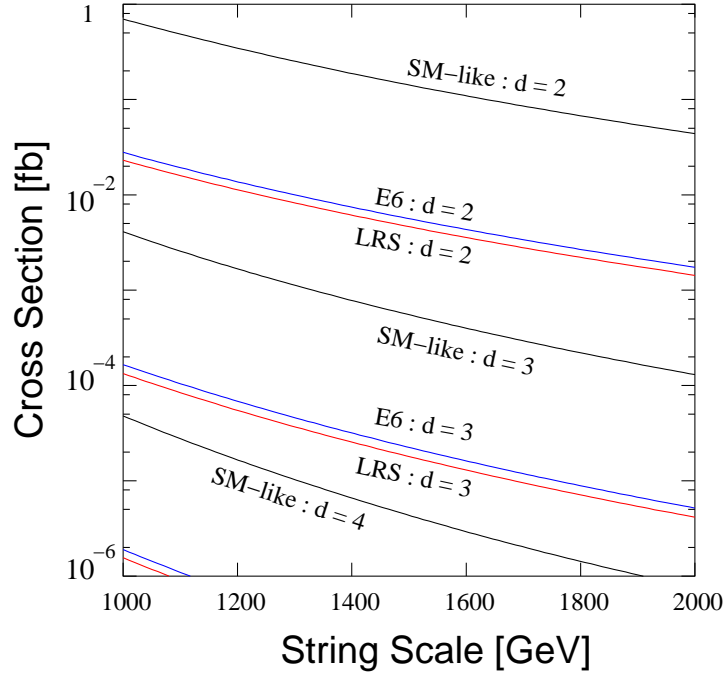


Figure 3. Cross-section for $e^+e^- \rightarrow \mu^+\mu^- \cancel{E}_T$ as a function of M_S , keeping $d = 2$ and $M_{Z'} = 250$ GeV. The black curves correspond to Model 1, i.e. the couplings of the Z' boson to fermions are identical to the couplings of the Z boson. Blue curves correspond to the E_6 -based Model 4 with $\beta = 0$, the last being chosen to correspond to large cross-section. Red curves correspond to a LR-symmetric Model 5 with $\alpha_{LR} \simeq \sqrt{2/3}$, which is also chosen to get the largest cross-section.

It immediately becomes clear from Figure 3 that the present process is viable at a 500 GeV collider, with an integrated luminosity of around 1000 fb^{-1} , only if we assume that $d = 2$ and M_S is not much greater than 1.8 GeV. For $d = 3$, one would require a much higher luminosity of at least 10^6 fb^{-1} in order to have observable effects. Higher values of d are simply not accessible at the planned energies and luminosities.

The above curves correspond to a Z' -boson mass of 250 GeV. For the same choice of mass, and with $d = 2$ and $M_S = 1$ TeV, we have plotted, in Figure 4, the distribution in dimuon invariant mass $M_{\mu\mu} = (p_{\mu^+} - p_{\mu^-})^2$ for all the five models in question.

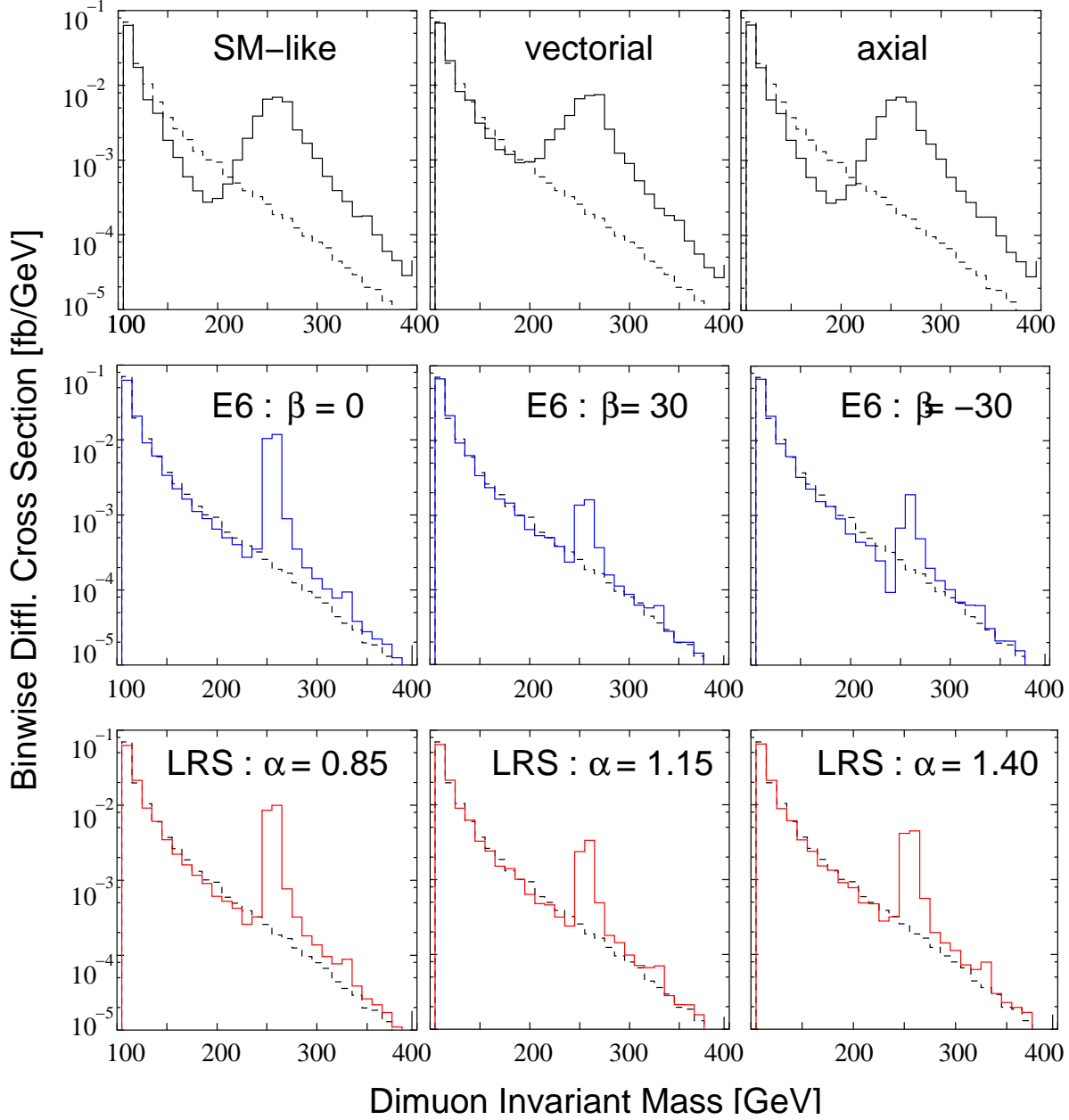


Figure 4. *Bin-wise distribution of the differential cross-section in dimuon invariant mass $M_{\mu\mu}$ in different models. The dashed histogram corresponds, in every case, to absence of any Z' resonance, i.e. to a SM on the brane. The top row illustrates the cases for Models 1, 2 and 3. The middle row illustrates Model 4 for different choices of mixing angle β , while the bottom row similarly illustrates the case of different choices of α_{LR} .*

In Figure 4, the dashed histogram represents the case when there is no Z' resonance in the given range, i.e. one observes only the SM on the brane. This falls off sharply as $M_{\mu\mu}$ increases because of the usual s -channel suppression far away from the photon and Z resonances. The presence of a Z' boson changes this behaviour dramatically, as shown by the solid histograms.

The first three, corresponding to Models 1, 2 and 3 respectively, have large and wide resonances, consistent with the larger width and couplings illustrated in Table 1 and Figure 2. The behaviour of ‘SM-like’ and ‘axial’ couplings for the Z' boson is very similar simply because the vector coupling of charged leptons to the Z boson is very small in the SM. There is a qualitative difference between these and a purely vectorial coupling, in that the latter does not show any destructive interference effects. More realistic results are shown in the blue and red histograms. The blue histograms correspond to the E_6 model with choices of $\beta = 0, \pi/6$ and $-\pi/6$ respectively. Though the model allows β to vary from $-\pi/2$ to $+\pi/2$, we found that the qualitative behaviour of the invariant mass distribution shows very little variation beyond $\beta = \pm\pi/6$. It is quite clear that $\beta = 0$ provides the largest resonances. For finite values of β the resonances look small in the figure, but are not actually so, since the ordinate is plotted on a logarithmic scale. Similar arguments hold for the red histograms in the bottom row, which correspond to Model 5, with different values of the coupling constant $\alpha_{LR} = 0.85, 1.15$ and 1.40 respectively, spanning the allowed range. As expected from the $1/\alpha_{LR}$ dependence shown in Table 1, the largest resonances correspond to the smallest value of α_{LR} .

We reiterate at this point that the actual point in the parameter space of the model incorporating Z' bosons is a matter of detail and our work does not focus on this. Figure 4 simply illustrates the fact that with quite realistic choices of parameters in this sector, we can expect large resonances in the dimuon mass distribution in the process $e^+e^- \rightarrow \mu^+\mu^- \cancel{E}_T$, provided the model is embedded in an ADD-like brane world scenario.

In all of the above analyses, the mass of the Z' boson was set to 250 GeV. It is natural to ask whether it would be possible to distinguish resonances when $M_{Z'}$ is larger and approaches the machine energy of 500 GeV. Obviously, in this case one would get smaller and broader resonances, which may not show such spectacular deviations from the SM expectations as shown in Figure 4. In this case, it is better to have a quantitative index, for which we have adopted a χ^2 fit to the line-shape. This has been done as follows: the differential cross-section has been calculated in 14 bins of 20 GeV each, starting from $M_{\mu\mu} = 200$ GeV to $M_{\mu\mu} = 480$ GeV. Denoting the cross-section in the i th bin by σ_i and choosing a luminosity $L = 10^3 \text{ fb}^{-1}$, we then calculate the number of events expected in each bin as $N_i = L\sigma_i$. We separately calculate the expected number for $N_i^{(SM)}$ and $N_i^{Z'}$, i.e. without and with the Z' resonance. If the expected number drops below unity, we set it to unity, to take care of random fluctuations and the fact that the law of large numbers is clearly not valid. The χ^2 is now calculated, assuming Gaussian errors (statistical only) $\delta N_i^{(SM)} = \sqrt{N_i^{(SM)}}$, using the

simple formula

$$\chi^2 = \sum_{i=1}^{14} \frac{(N_i^{Z'} - N_i^{(SM)})^2}{N_i^{(SM)}} \quad (4)$$

The value of this χ^2 is a measure of the deviation of the line-shape in $M_{\mu\mu}$ from the SM expectations and consequently falls as the resonances become smaller. For $\chi^2 < 23.7$, the line-shape is consistent with Gaussian random fluctuations in the SM at 95% confidence level (C.L.), which means that this value of χ^2 corresponds to the 95% discovery limit of the resonance.

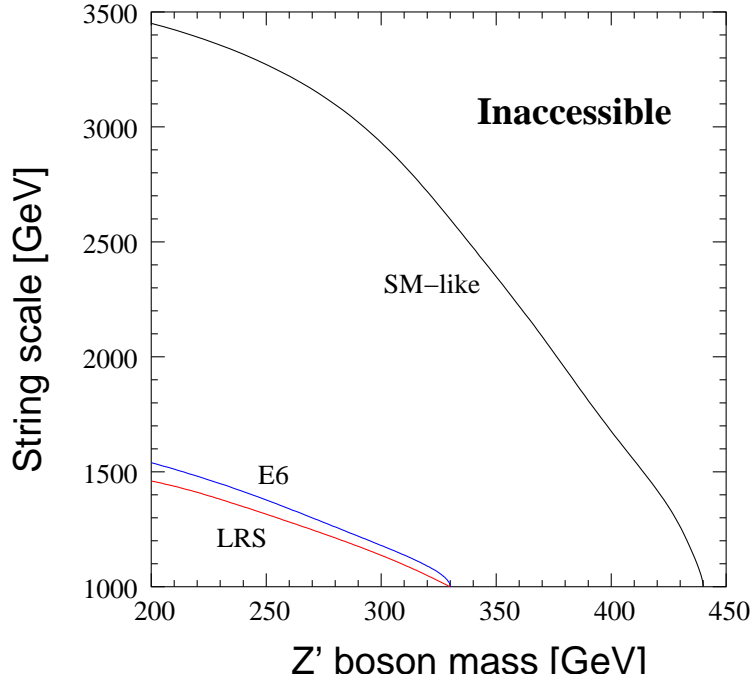


Figure 5. 95% C.L. discovery limits in the M_S – $M_{Z'}$ plane corresponding to three different models. The black curve corresponds to a Z' boson with SM-like couplings to fermions. The blue curve corresponds to an E_6 -based model with $\beta = 0$ and the red curve corresponds to a LR symmetric model with $\alpha_{LR} \simeq \sqrt{2/3}$.

In Figure 5, we have plotted these 95% C.L. discovery limits in the M_S – $M_{Z'}$ plane, the region *below* the curve being accessible to a 500 GeV linear collider with 10^3 fb^{-1} luminosity. The three curves all correspond to $d = 2$ and, respectively, Model 1 (black), Model 4 (blue) with $\beta = 0$ and Model 5 (red) with $\alpha_{LR} = 0.85$, these being (as we have seen) the choices which lead to the largest cross-sections. As expected from the large cross-sections in Figure 3, the discovery limits are the most robust in the (unphysical) case of Model 1, and the ones for the more realistic cases look disappointing by contrast. Nevertheless, it should be possible, for a string scale not much larger than a TeV, to detect Z' resonances all the way up to nearly 330 GeV. Given the kinematic constraints at a machine energy of 500 GeV, this is quite a reasonable effect. Moreover, as stated above, the purpose of this work is to highlight the

possibility of exciting resonances of perhaps unknown nature, and not to focus on the details of models with Z' bosons.

In this paper, therefore, we have investigated the possibility that, at a 500 GeV e^+e^- collider, invisible graviton radiation in a brane world scenario could provide a useful tool to discover low-lying resonances coupling to e^+e^- and $\mu^+\mu^-$ pairs. Not only are such resonances predicted in extensions of the standard electroweak model, but some might be low-lying stringy excitations arising in a theory with TeV strings. We have explored the collider phenomenology of this process by focussing on extra Z' bosons and showed that reasonably optimistic discovery limits are predicted in two of the more popular models. In so doing, we have also established the methodology for investigation of this particular signal. It may be noted that at a 500 GeV e^+e^- collider, one of the easiest processes to look for will be a hard muon pair with substantial missing energy, and we shall surely have data on this when the machine actually runs. The possibility that a new resonant state will be discovered — or, at least, confirmed — in this process is by no means a far-fetched one, and this is the substance of the present work. Quite obviously, there are severe limitations due to the limited energy and luminosity available at the machine in question, and one could carry out a more extensive study if, for example, the collisions took place at $\sqrt{s} = 2$ TeV and an integrated luminosity of 10^6 fb^{-1} could be achieved[12]. However, we feel that it is premature to carry out any numerical analysis based on such machine parameters. Our point is sufficiently conveyed by the rather spectacular resonant structures shown in, for example, Figure 4, and a study of the remaining aspects could await the development of a detailed machine design for the International Linear Collider.

The authors acknowledge useful discussions with S.K. Rai. SR acknowledges the hospitality of the Institute of Physics, Bhubaneswar, India, where a part of this work was done. The work of SS was funded by the Department of Science and Technology, Government of India.

References

- [1] For a recent status report, see, for example, K. Moenig, *Acta Phys.Polon.* **B36**, 3327 (2005).
- [2] See, for example, E. Accomando *et al.*, *Phys.Rept.* **299**, 1 (1998).
- [3] T. Buanes, E.W. Dvergsnes and P. Osland, *Eur.Phys.J.* **C35**, 555 (2004);
N.K. Mondal *et al.*, *Pramana* **63**, 1331 (2004).
- [4] N. Arkani-Hamed, S. Dimopoulos and G.R. Dvali, *Phys.Lett.* **B429**, 263 (1998) and
Phys.Rev. **D59**, 086004 (1999);
I. Antoniadis, N. Arkani-Hamed, S. Dimopoulos and G.R. Dvali, *Phys.Lett.* **B436**, 257 (1998).
- [5] S. Cullen, M. Perelstein and M.E. Peskin, *Phys.Rev.* **D62**, 055012 (2000).
- [6] G.F. Giudice, R. Rattazzi and J.D. Wells, *Nucl.Phys.* **B544**, 3 (1999).
- [7] T. Han, J.D. Lykken and R.-J. Zhang, *Phys.Rev.* **D59**, 105006 (1999).
- [8] See, for example, J.A.M. Vermaseren, math-ph/0010025.
- [9] See, for example, Y. Uehara, *Mod.Phys.Lett.* **A17**, 1551 (2002).
- [10] S. Cullen and M. Perelstein, *Phys.Rev.Lett.* **83**, 268 (1999);
V.D. Barger *et al.* *Phys.Lett.* **B461**, 34 (1999).
- [11] M. Dittmar, A.-S. Nicollerat and A. Djouadi, *Phys.Lett.* **B583**, 111 (2004).
- [12] See, for example, the report by the CLIC Physics Working Group (E. Accomando *et al.*),
hep-ph/0412251.